Separation Science and Technology
Publication details, including instructions for authors and subscription information:
http://www.informaworld.com/smpp/title~content=t713708471

Feasibility Study of Dielectrical Field-Flow Fractionation

Joe M. Davis[a]; J. Calvin Giddings[a]
[a] Department of Chemistry, University of Utah, Salt Lake City, Utah

To cite this Article Davis, Joe M. and Giddings, J. Calvin(1986) 'Feasibility Study of Dielectrical Field-Flow Fractionation', Separation Science and Technology, 21: 9, 969 — 989
To link to this Article: DOI: 10.1080/01496398608058390
URL: http://dx.doi.org/10.1080/01496398608058390

SEPARATION SCIENCE AND TECHNOLOGY, 21(9), pp. 969-989, 1986

Feasibility Study of Dielectrical Field-Flow Fractionation

JOE M. DAVIS and J. CALVIN GIDDINGS

DEPARTMENT OF CHEMISTRY
UNIVERSITY OF UTAH
SALT LAKE CITY, UTAH 84112

Abstract

The possible use of dielectrophoretic forces for the development of a new subtechnique of field-flow fractionation (FFF) termed dielectrical FFF is examined. Dielectrical FFF is based on the dielectrophoresis of neutral particles in the nonuniform electric field of an annular channel (or charged coaxial capacitor). The feasibility of the subtechnique is assessed by estimating the magnitudes of retention ratio R predicted from theory for select species representative of several classes of particle/fluid mixtures. Minimum attainable R values are calculated using estimates of the maximum electric field strengths applicable to the mixtures. Calculations show that the dielectrophoretic force is strong enough to retain and separate ultrahigh-molecular-weight polymers and submicron-diameter particles dissolved or suspended in organic liquids of high dielectric constant. Evidence suggests that pearl-chain formation may impose a fundamental limitation on particle retention at the inner cylinder of the annular channel, especially in aqueous suspensions.

INTRODUCTION

Field-flow fractionation (FFF) is a family of chromatographic-like separation methods well adapted to the analytical-scale fractionation and characterization of macromolecules and small colloidal particles, including proteins, viruses, latex samples, emulsions, polymers, cells, and many other similar materials. Separation by FFF arises because components are differentially transported by laminar flow through an open channel of thin dimensions (usually 50–500 μm). In FFF, component particles are localized near one channel wall (the accumulation wall) by an external field or gradient which is applied perpendicular to the flow direction (see

0149-6395/86/2109-0969$3.50/0

Fig. 1A). Soon after sample injection, each species forms a steady-state particle cloud (or zone) whose thickness is determined by the interplay of the field-induced force on the particles (which favors cloud formation) and particle diffusion (which opposes cloud formation). Component zones localized near the wall are carried less rapidly by flow than are less localized zones because the fluid velocity approaches zero at the walls (Fig. 1A). The principles of FFF have been described in more detail elsewhere (*1–3*).

The simplicity of the FFF system has facilitated derivation of general equations predicting the behavior of component zones in FFF systems. From these equations, characteristic physicochemical properties of constituent particles can be calculated from experimental measurements. Furthermore, such equations serve as useful guidelines with which to evaluate the promise and limitations of new FFF subtechniques.

The different subtechniques of the FFF family are distinguished principally by the type of field or gradient used. Different fields are applicable to different kinds of particles over different ranges of particle size and provide different levels of selectivity. For each new field a new physicochemical property of constituent particles can be measured. Thus, any new and viable subtechnique will serve to extend the FFF methodology into new areas and will reflect more diverse properties.

Presently, thermal (*4*), sedimentation (*5*), electrical (*6*), flow (*7*), and magnetic (*8*) fields or gradients have been successfully used in FFF systems to fractionate and characterize a wide variety of macromolecules and particles. The possibility of using shear (*9*) and sedimentation hyperlayer (*10*) (alternatively called sedimentation-flotation focusing (*11*)) forces has also been considered and found promising.

In this paper we develop criteria for a new FFF subtechnique based on dielectrophoresis, or the translation of neutral particles (or molecules) in a spatially nonuniform electric field. Dielectrophoresis occurs because the nonuniform field polarizes (induces charge separation in) any exposed particle and exerts unequal forces on the various charge elements distributed over the particle, resulting in translation.

Alternative methods of separation based on the use of dielectrophoretic forces include dielectric levitation (*12–16*) and filtration (*17–22*). In dielectric levitation the spatial separation of different particle types suspended in organic liquids or aqueous media can be selectively adjusted by choice of the suspending medium, the electric field strength and frequency, and the electrode configuration and orientation. In dielectric filtration, organic or aqueous suspensions of particulates are pumped or gravity-fed through an annular or annularlike channel across which an electric field is applied. The proper choice of conditions can

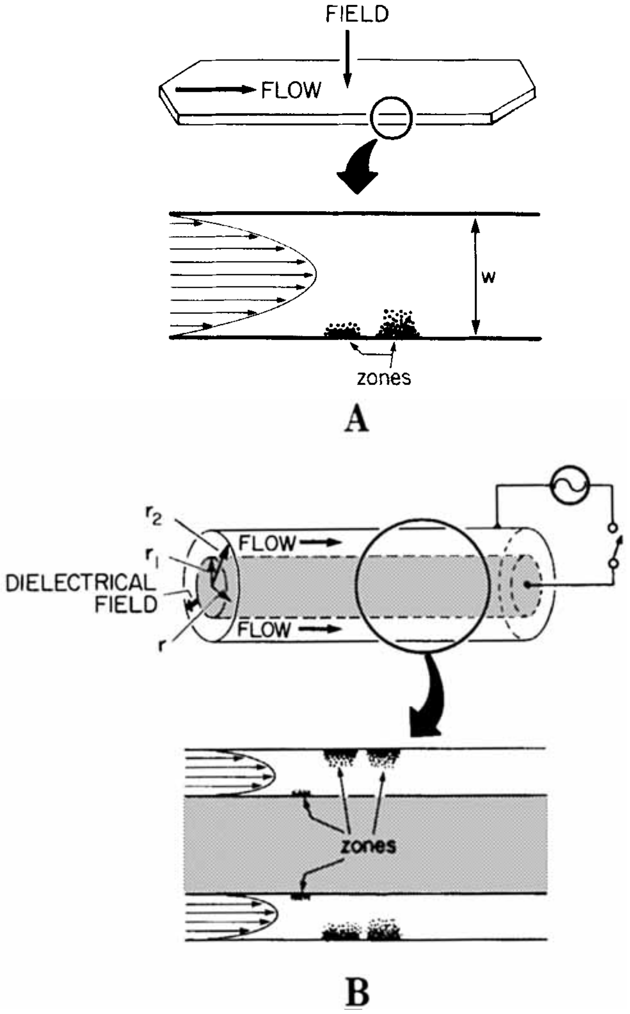

FIG. 1. (A) Open parallel-plate channel (OPPC) traditionally used in FFF. (B) Annular channel (ANNC) for dielectrical FFF.

favor either the enrichment or depletion of particles in the fluid. Dielectric filtration is sometimes used to purify organic liquids contaminated by particulates and fines.

The dielectrophoretic force F depends on a number of experimentally controllable parameters, among them the electrical permittivity and conductivity of the carrier fluid, the electrode configuration, and the frequency and magnitude of the electric field. It appears that a judicious choice of these parameters will yield a sufficiently large F to enable the fractionation of various particle mixtures under a variety of conditions. One can envision a broadening of the range of fractionation by implementing dielectrical FFF in a field-programmed mode in which the electric field strength or frequency (or both) is varied with time. The potential versatility of the proposed subtechnique is thus considerable.

The feasibility of dielectrical FFF is characterized here principally by the magnitudes of retention ratio R, equal to the ratio of the average velocity of the particle cloud to the average fluid velocity. Values of R are predicted from theory for select species representative of three classes of particle/fluid mixtures, namely dissolved polymers in organic solvents, organic particle suspensions, and aqueous particle suspensions. The smallest attainable R (or highest retention) is ultimately limited by the magnitude of electric field strength E, which if larger than some threshold strength E^t results in unfavorable or unacceptable conditions for fractionation. Several factors can determine E^t for a given particle/fluid mixture, including the dielectric breakdown of the mixture, the field-induced association of particles (which is discussed below), the Joule heating and thermal convection of the channel contents, or charge injection (*23*), which may electrostatically mix the fluid and zones. The criterion we use to decide if dielectrical FFF is a potential separation method for these classes of mixtures is that R must be adequately small, i.e., $R \leqslant 0.5$, for E values beneath the E^t threshold. (While the R's of all components need not be small, efficient multicomponent separations are not feasible unless nearly all R's are below 0.5.)

The mutual polarization and attraction of particles having larger complex electrical permittivities than the surrounding fluid result in the association of particles into linear complexes called "pearl chains" (*23*) if $E \geqslant E^p$, where E^p is the threshold strength for pearl-chain formation (or mutual dielectrophoresis) in that particle/fluid mixture. When such chains form, the size selectivity of the dielectrophoretic force is lost and large chains of particles (instead of individual particles) respond to and align with the electric field. If the particle chains are not broken up by the shear stresses attributable to the laminar flow of carrier fluid, their extensive length (which can be as much as 50–200 μm for chains composed of submicron-diameter particles (*23*)) will clearly result in severely distorted transport in the FFF system.

For the purposes of this paper we consider E to be limited primarily by the dielectric strength E^d or the pearl-chain-formation strength E^p of the mixture. Thus the threshold field strength E^t, above which practical operation is not possible, is considered to be the lesser of the two quantities E^d and E^p.

A number of electrode configurations external to the walls of the open parallel-plate channel or OPPC (see Fig. 1A) traditionally used in FFF can be proposed to generate nonuniform electric fields, but the mathematical descriptions of these fields and their effects would generally not be simple. We consider here, alternatively, the use of a coaxial capacitor, which is equivalent to an annular channel or ANNC in which the electrodes are the channel walls. The ANNC has inner radius r_1 and outer radius r_2; a potential difference is applied across the gap thickness $w = r_2 - r_1$, as shown in Fig. 1B, to produce a nonuniform E. The field strength and dielectrophoretic force are well defined for this geometry, allowing us to evaluate R using a retention theory recently developed for ANNCs (*24*). (An alternative dielectrical FFF channel is an approximation to the isomotive electrode cell (*19, 23*).)

Dielectrophoresis is observed in both dc and ac fields. We consider here only ac fields to avoid complications associated with dc fields, such as electrode polarization and electrophoresis.

THEORY

We simplify our analysis by assuming that all particles and molecules are uniform spheres. We wish to calculate the steady-state ac-dielectrophoretic force F on a sphere of volume V and complex electrical permittivity $\varepsilon_p^* = \varepsilon_p - i\sigma_p/\omega$. When such a sphere is immersed in an unbounded fluid of complex electrical permittivity $\varepsilon_f^* = \varepsilon_f - i\sigma_f/\omega$ through which passes an asymmetric electric field $E = E_s(q)e^{j\omega t}$ oscillating with angular frequency ω, the dipolar approximation to F is (*23, 25–27*)

$$F = \frac{3}{2}\theta' V\varepsilon_f \mathrm{Re}\left(\frac{\varepsilon_p^* - \varepsilon_f^*}{\varepsilon_p^* + 2\varepsilon_f^*}\right)\nabla E_s^2 = \frac{3}{2}\theta' V\varepsilon_f\left(\frac{\varepsilon_p - \varepsilon_f}{\varepsilon_p + 2\varepsilon_f} + \frac{3(\varepsilon_f\sigma_p - \varepsilon_p\sigma_f)}{(\varepsilon_p + 2\varepsilon_f)(\sigma_p + 2\sigma_f)(1 + (\omega\tau_f)^2)}\right)\nabla E_s^2 \tag{1}$$

where ε_p and σ_p (ε_f and σ_f) are the electrical permittivity and conductivity of the particle (fluid), $E_s(q)$ denotes the cyclical maximum value of field strength E at the generalized coordinate position q, t is time, $\mathrm{Re}(\zeta)$ designates the real part of any arbitrary complex number ζ, $i = \sqrt{-1}$, and τ_f is the time constant that characterizes the duration of a transient component of the ac-dielectrophoretic force (which merits consideration only when $\omega \simeq 1/\tau_f$ and $t < \tau_f$ *(26)*):

$$\tau_f = \frac{\varepsilon_p + 2\varepsilon_f}{\sigma_p + 2\sigma_f} \tag{2}$$

In Eq. (1), coefficient $\theta' = 0.5$; the product $\theta' \nabla E_s^2$ could alternatively be written as $\nabla E_{\mathrm{rms}}^2$, where E_{rms} is the root-mean-square (rms) value of E. Quantity ∇E_s^2 could also be written as $2E_s \nabla E_s$. The latter form more clearly expresses the physical dependence of F on the electric field E_s, which polarizes the particle, and the field gradient ∇E_s, which measures the relative difference in electrical force on the charge elements distributed over the particle.

Alternatively, and more simply, Eq. (1) can be written as the product of three terms:

$$F = Vg\nabla E_s^2 \tag{3}$$

where volume V is generally the only parameter depending on particle size, ∇E_s^2 accounts entirely for the effects of the electrical field, and parameter g,

$$g \equiv g(\varepsilon_p^*, \varepsilon_f^*) \equiv \frac{3}{2}\,\theta' \varepsilon_f \mathrm{Re}\left(\frac{\varepsilon_p^* - \varepsilon_f^*}{\varepsilon_p^* + 2\varepsilon_f^*}\right) \tag{4}$$

incorporates all of the intensive properties of the particle and fluid media that are relevant to dielectrophoretic force. Particles migrate toward the region of increasing E if the function g is positive (positive dielectrophoresis) and decreasing E if g is negative (negative dielectrophoresis).

The maximum value $E_s(r)$ of field strength E in an ANNC can be written as a function of radial coordinate r (see Fig. 1B) *(23)*:

$$E_s = E_1 r_1 / r \tag{5}$$

where E_1 is the maximum field strength E_s in the system, found at $r = r_1$, the inner cylinder. Thus

$$\nabla E_s^2 = -2E_1^2 \frac{r_1^2}{r^3} \tag{6}$$

The combination of Eqs. (3), (4), and (6) allows us to express force F in terms of E_1, which is limited to values less than E^t as noted earlier.

The general retention theory for ANNCs shows that retention ratio R can be expressed in terms of F as a definite integral (see Eq. 14) which depends on the parameters

$$\lambda = kT/|W| = kT/\left|\int_{r_1}^{r_2} F\,dr\right| \tag{7}$$

and

$$\rho_1 = r_1/r_2 \tag{8}$$

where kT is the thermal energy of the system and W is the work required to transport a particle across the gap $w = r_2 - r_1$ (*24*).

Substituting Eqs. (3) and (6) into Eq. (7), we find that

$$\lambda = \frac{kT}{|g|VE_1^2(1 - \rho_1^2)} \tag{9}$$

This general λ equation can be explicitly written for different particle types by specifying the function g and particle volume V. For a polymer of molecular weight M and density ρ, λ becomes

$$\lambda = \frac{4\rho \boldsymbol{R}T}{3M\varepsilon_f\left|\mathrm{Re}\left(\dfrac{\varepsilon_p^* - \varepsilon_f^*}{\varepsilon_p^* + 2\varepsilon_f^*}\right)\right|E_1^2(1 - \rho_1^2)} \tag{10}$$

where $\boldsymbol{R}$ is the gas constant and θ' is assigned the value 0.5. (In deriving Eq. (10), the polymer molecule is assumed to be a sphere of pure polymeric material in place of the more open structure representative of the random coil polymer in solution.)

For a spherical particle of radius a, λ assumes the form

$$\lambda = \frac{kT}{\pi a^3\varepsilon_f\left|\mathrm{Re}\left(\dfrac{\varepsilon_p^* - \varepsilon_f^*}{\varepsilon_p^* + 2\varepsilon_f^*}\right)\right|E_1^2(1 - \rho_1^2)} \tag{11}$$

Equations (9)–(11) apply, as suggested earlier, only when the maximum inner-cylinder field strength E_1 is no greater than E^t. Hence the threshold parameter λ^t that determines the minimum attainable R for a given ε_p^*, ε_f^*, V, and ρ_1 is obtained by equating E_1 to E^t. In particular, the smallest attainable λ value limited by the dielectric strength E^d of the suspension, λ^d, is obtained by equating E_1 to E^d. Likewise, the smallest λ obtainable under pearl-chain limitations is found by substituting E^p for E_1.

The maximum practical field strength E^p, above which spherical particles form pearl chains, is (*23*, *28*, *29*)

$$E^p = 1.7\left|\frac{\varepsilon_p^* + 2\varepsilon_f^*}{\varepsilon_p^* - \varepsilon_f^*}\right|\left(\frac{4\pi kT}{3\theta'\varepsilon_f V}\right)^{1/2} \tag{12}$$

where for any complex number ζ, |ζ| denotes its modulus. Pearl-chain formation is thus expected to begin near the inner cylinder of the ANNC when the field strength at that boundary reaches the level $E_1 = E^p$. Substituting this expression into Eq. (9) and expressing g explicitly, we find that the pearl-chain limited λ is

$$\lambda^p = \frac{0.0551}{1 - \rho_1^2}\,\frac{|(\varepsilon_p^* - \varepsilon_f^*)/(\varepsilon_p^* + 2\varepsilon_f^*)|^2}{|\mathrm{Re}((\varepsilon_p^* - \varepsilon_f^*)/(\varepsilon_p^* + 2\varepsilon_f^*))|} \tag{13}$$

and is independent of particle volume V. Thus, while the experimental λ for a given particle type is inversely proportional to V, pearl chains form more readily (see Eq. 12) at large V. Consequently, increasing particle size forces a reduction in field strength whose effect on λ exactly offsets that of V. (For a particle mixture, λ^p would be the limiting λ for the largest particle; the smaller particles would have λ's increasing in inverse proportion to V.)

The dielectrical FFF retention ratio R is calculated from the above expressions and the definite integral (*24*)

$$R = \frac{2}{\phi}\,\frac{\displaystyle\int_{\alpha/\rho_1^2}^{\alpha} \exp(\mp u)\left(\frac{1}{u}\right)^2\left(1 - \frac{\alpha}{u} + \frac{\theta}{2}\ln\frac{u}{\alpha}\right)du}{\displaystyle\int_{\alpha/\rho_1^2}^{\alpha} \exp(\mp u)\left(\frac{1}{u}\right)^2 du} \tag{14}$$

where

$$\alpha = \frac{\rho_1^2}{\lambda(1 - \rho_1^2)} \tag{15}$$

$$u = \alpha r_2^2/r^2 \tag{16}$$

$$\theta = \frac{1 - \rho_1^2}{\ln \rho_1} \tag{17}$$

and

$$\phi = 1 + \rho_1^2 + \theta \tag{18}$$

The upper and lower signs in the exponential factor of Eq. (14) indicate that R differs for outer-wall and inner-wall retention, respectively. The integrals in Eq. (14) cannot in general be evaluated analytically, but when $\lambda \ll 1$, the R expression reduces to (*24*)

$$R_{\text{in}} \simeq \frac{kT}{g\phi E_1^2 V} |2\rho_1^2 + \theta| \tag{19}$$

and

$$R_{\text{out}} \simeq \frac{kT}{|g|\rho_1^2 \phi E_1^2 V} (2 + \theta) \tag{20}$$

where R_{in} and R_{out} are the inner- and outer-wall retention ratios. The λ ranges over which these approximations are valid depend on ρ_1 and are given elsewhere (*24*).

We observe that some experimental aspects of the dielectrophoretic phenomenon are not accounted for in the present ANNC retention theory for R and merit mention here. First, a spherical particle subject to dielectrophoresis in ionic media commonly rotates slowly (e.g., $\simeq$ 10 Hz), most likely due to the adherence of ions to the particle surface and the resultant induction by the electric field of a rotational torque on the particle (*23*). Second, a freely rotating nonspherical particle (e.g., an ellipsoid) is subject to a frequency-dependent orientation in an electric field because the electrical energy stored in the particle is partitioned among the particle's three principal axes, the relative partitioning is frequency-dependent, and the minimum-energy axis of the particle aligns with the field (*23, 30, 31*). The influences of these two phenomena on zone migration (and thus R) are assumed to be second order and are consequently not treated here.

NUMERICAL

Table 1 reports the relative dielectric constants (the electrical permittivities divided by the permittivity of free space), electrical conductivities, and dielectric strengths (the field strengths at which dielectric

TABLE 1
Dielectrical Properties of Select Substances[a]

Substance	Dielectric constant (dimensionless)	Conductivity (mho/m)	Dielectric strength[a] (V/m)
Polyethylene (ρ = 0.95 g/cm^3) (*34*)	2.28	6.3×10^{-12} (*35*)	1.8×10^7 5.3×10^8 at 50°C (*33*))
Cellulose acetate (*34*) (ρ = 1.55 g/cm^3)	5.1	10^{-8} to 10^{-11}	$1.0\text{–}1.4 \times 10^7$
Fused silica (*34*)	3.8	10^{-10}	1.6×10^7
Porcelain (*34*)	5.36		2×10^6 to 2×10^7
Al_2O_3 (*34*)	8.83	$<10^{-9}$	$2\text{–}6 \times 10^6$
TiO_2 (*34*)	14–110	10^{-12} to 10^{-18}	$3.9\text{–}8.3 \times 10^6$
p-Xylene	2.27	7.6×10^{-14}	
n-Hexane	1.88	$<1 \times 10^{-14}$	$>5 \times 10^7$ (*35*)
Methyl ethyl ketone (MEK)	18.51	3.6×10^{-7}	
Dimethylsulfoxide (DMSO)	46.68	2×10^{-7}	
Water	78.33	5.9×10^{-6}	
Formamide	111.0	2×10^{-5}	
N-Methylformamide	182.4	8×10^{-5}	

[a] Quantities vary a few percent from cited values over the frequency range ~10–10^4 Hz. Dielectric strengths are rms values. Temperature range: 20–25°C unless otherwise noted. Dielectric strengths of polar and nonpolar organic liquids are typically 10^8 V/m (*35*). Data are cited from Ref. *32* unless otherwise noted.

breakdown occurs) of several substances chosen as representative components of the three particle/fluid mixtures examined in this study. These values generally vary only a few percent over a wide range ($10-10^4$) of frequencies.

Table 2 reports the estimated dielectric strengths E^d and pearl-chain-formation strengths E^p used for calculations on the particle/fluid mixtures characterized here; the threshold field strength E^t of each system was chosen as the lesser of the two appropriate values. The dielectric strengths of these mixtures are assumed generally to be limited by the dielectric strengths of the suspended or dissolved particles. Conservative (low) values have been chosen for E^d because of uncertainties on how these limitations would apply in practical FFF systems.

For each mixture, values of threshold parameter λ^t were calculated for various V and ρ_1 values using Eq. (10) or (11), the appropriate inner-cylinder field strength $E_1 = E^t$, the cyclical frequency $\nu = \omega/2\pi = 10{,}000$ Hz, and $T = 300$ K. Retention ratio R was then calculated from these λ^t and ρ_1 values by integrating Eq. (14) numerically, using Simpson's rule.

RESULTS AND DISCUSSION

We first consider the feasibility of fractionating nonaqueous suspensions of colloidal particles using dielectrical FFF. As observed in the Introduction, dielectrophoresis is sometimes used to remove particulate impurities from organic fluids. Of increasing interest is the fractionation and characterization of various particulate materials suspended in such liquids, such as the organic and inorganic contaminants in coal liquids. Dielectrical FFF is a promising method for fractionating such mixtures, as shown below.

Since force F, Eq. (1), increases with fluid permittivity ε_f, the smallest λ^t's and R's attainable for fixed ρ_1, E_1, V, and ε_p^* are found by suspending particulate materials in liquids of high dielectric constant. Particles suspended in such liquids are generally subject to negative dielectrophoresis (i.e., outer-wall retention) because $\varepsilon_f^* > \varepsilon_p^*$, and the threshold strengths E^t of these mixtures are determined principally by the dielectric strengths E^d. We choose here $E^d = 1.4 \times 10^6$ V/m ($E^d_{\mathrm{rms}} = 1.0 \times 10^6$ V/m or 1.0 V/μm) since the dielectric strengths of many particulate types are only slightly greater than this value (see Table 1).

Figure 2 is a plot of log R vs ρ_1 determined as detailed above for the suspension of 0.3-μm-diameter spheres of fused silica and Al_2O_3 in the three organic liquids, *p*-xylene, methyl ethyl ketone (MEK), and *N*-methylformamide. Both particulate types are subject to outer-wall

TABLE 2
Electric Field Strengths E^d, E^p, and E^t for Select Particle/Fluid Mixtures[a]

Particle/fluid mixture	Estimated E^d (V/m)	E^p, calculated from Eq. (12) (V/m)	Threshold E^t (V/m)
Silica/*p*-xylene	1.4×10^6	3.1×10^6	1.4×10^6
Silica/MEK	1.4×10^6	[b]	1.4×10^6
Silica/*N*-methylformamide	1.4×10^6	[b]	1.4×10^6
Al_2O_3/*p*-xylene	1.4×10^6	1.2×10^6	1.2×10^6
Al_2O_3/MEK	1.4×10^6	[b]	1.4×10^6
Al_2O_3/*N*-methylformamide	1.4×10^6	[b]	1.4×10^6
Silica/DMSO	1.4×10^6	[b]	1.4×10^6
Silica/formamide	1.4×10^6	[b]	1.4×10^6
Al_2O_3/DMSO	1.4×10^6	[b]	1.4×10^6
Al_2O_3/formamide	1.4×10^6	[b]	1.4×10^6
Cellulose acetate/*N*-methylformamide	1.4×10^7	[b]	1.4×10^7
Cellulose acetate/DMSO	1.4×10^7	[b]	1.4×10^7
Polyethylene/*n*-hexane	1.4×10^7	$>2.8 \times 10^7$[c]	1.4×10^7

[a] MEK = methyl ethyl ketone; DMSO = dimethylsulfoxide.
[b] Pearl-chain formation not expected.
[c] For $M \leqslant 10^9$ g/mol.

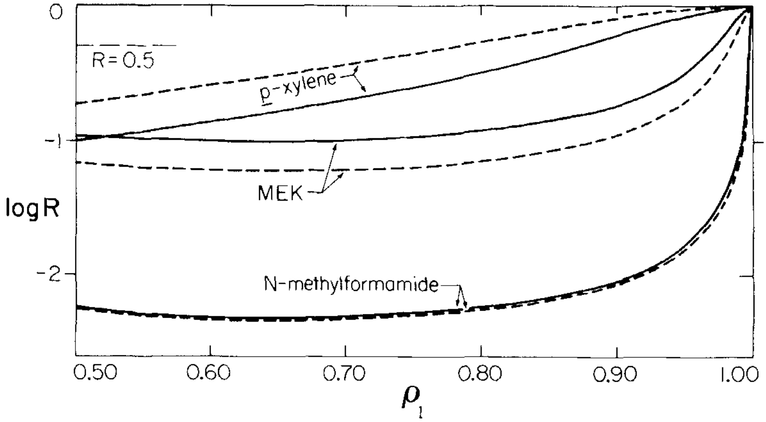

FIG. 2. Plot of log R vs ρ_1 for 0.3-μm-diameter spheres of fused silica (dashed lines) and Al_2O_3 (solid lines) suspended in *p*-xylene, methyl ethyl ketone (MEK), and *N*-methylformamide. $E^t = 1.4 \times 10^6$ V/m; $\nu = 10{,}000$ Hz.

retention in the latter two liquids and to inner-wall retention in *p*-xylene; the threshold strength E^t of the Al_2O_3/*p*-xylene mixture is determined by E^p instead of E^d (see Table 2). The figure illustrates the general trend in which retention increases (i.e., R decreases) as the fluid permittivity is increased, irrespective of the wall of accumulation. Furthermore, under optimal conditions, $\varepsilon_f^* \gg \varepsilon_p^*$ and force F approaches a limiting value for fixed ε_f^*, ρ_1, V, and E_1 that is largely independent of ε_p^* (note that the R values for Al_2O_3 and silica suspended in *N*-methylformamide are nearly identical despite a more than twofold difference in ε_p).

The influence of ρ_1 on R is also illustrated by Fig. 2. We observe that R approaches unity and λ, Eq. (9), approaches infinity as ρ_1 approaches unity because, at fixed r_2 (or r_1), the gap thickness w approaches zero in this limit and the term $|W|$ in Eq. (7) goes to zero. The function R_{in} decreases (upper pair of curves) with decreasing ρ_1, principally because w and thus $|W|$ increase as ρ_1 decreases at fixed r_2. The function R_{out} (two lowest pairs of curves) is smallest for intermediate ρ_1 values because $|W|$ goes through a maximum as ρ_1 decreases. A rather large ρ_1 range is found over which R_{out} varies only slightly from its minimum value.

Figure 3 is a plot of R vs particle diameter $2a$ determined for suspensions of fused silica and Al_2O_3 spheres in the three fluids, dimethylsulfoxide (DMSO), formamide, and N-methylformamide. Values of R (in all cases corresponding to outer-wall retention) were calculated for each of the six suspensions assuming $\rho_1 = 0.75$ (e.g., $r_1 = 1.5$ mm, $r_2 = 2.0$ mm, and $w = 500$ μm) and $\rho_1 = 0.90$ (e.g., $r_1 = 2.29$ mm, $r_2 = 2.54$ mm, and $w = 250$ μm). The figure shows that outer-wall retention is clearly favored by the selection of a high permittivity fluid and of a relatively small ρ_1 value. We observe that under favorable conditions, particles having diameters down to 0.06 μm can apparently be favorably retained ($R \leqslant 0.5$).

Two experimentally controllable parameters on which force F depends are the fluid conductivity σ_f and angular frequency ω of the electric field. If F is maximized for a given E_1, V, and ρ_1 by choosing a high permittivity liquid, for which typically $\varepsilon_f \gg \varepsilon_p$, little change in F (and R) is expected as σ_f or ω is varied. This invariance can be understood if we recognize that the real part of the complex factor in Eq. (1), which is bound by the limits

$$-0.5 \leqslant \mathrm{Re}\left(\frac{\varepsilon_p^* - \varepsilon_f^*}{\varepsilon_p^* + 2\varepsilon_f^*}\right) \leqslant 1 \qquad (21)$$

approaches the limit, −0.5, for any σ_f or ω when $\varepsilon_f \gg \varepsilon_p$. Hence, an

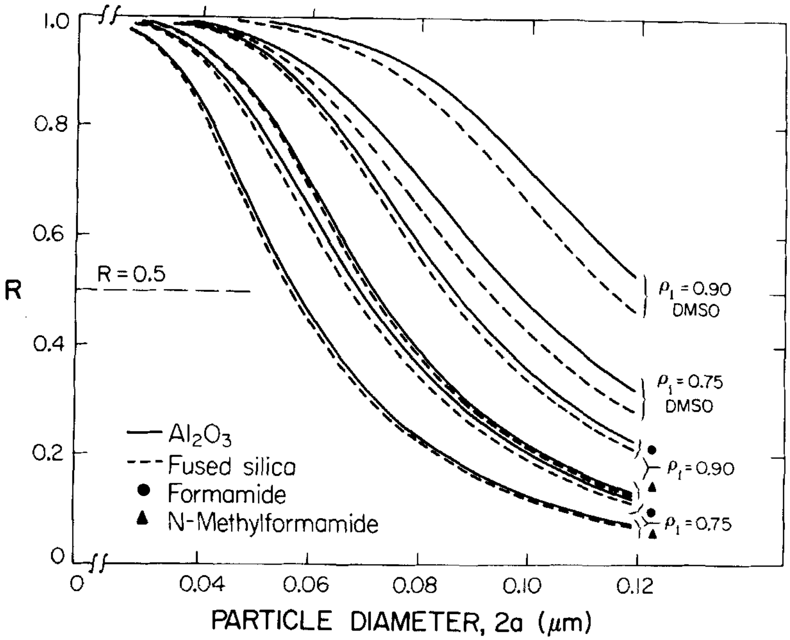

FIG. 3. Plot of R vs particle diameter $2a$ for spheres of fused silica (dashed lines) and Al_2O_3 (solid lines) suspended in dimethylsulfoxide (DMSO), formamide, and *N*-methylformamide. $E^t = 1.4 \times 10^6$ V/m; $\nu = 10{,}000$ Hz.

optimized dielectrical FFF experiment will largely be independent of frequency and fluid conductivity.

We now briefly assess the feasibility of polymer fractionation by dielectrical FFF. The large dielectric strength $E^d = 1.4 \times 10^7$ V/m was chosen as a representative value for typical polymer solutions (see Table 1). Figure 4 is a plot of R vs molecular weight M in g/mol predicted for the polymer cellulose acetate dissolved in *N*-methylformamide and in DMSO and for polyethylene dissolved in *n*-hexane, assuming $\rho_l = 0.75$. Adequate retention ($R \leqslant 0.5$) is attainable in both polar solvents for 10^6- to 10^7-molecular-weight cellulose acetate, but the molecular weight of polyethylene must be greater than ~2.7×10^8 g/mol to retain adequately this polymer in *n*-hexane, largely because $\varepsilon_p^* \simeq \varepsilon_f^*$ and ε_f is relatively small. Polymers having molecular weights much less than 10^6 g/mol are inadequately retained under the best of conditions principally because force F is volume-dependent (see Eq. 1) and the volume V occupied by a polymer molecule is quite small, even for large M (e.g., $V = 1.66 \times 10^{-17}$

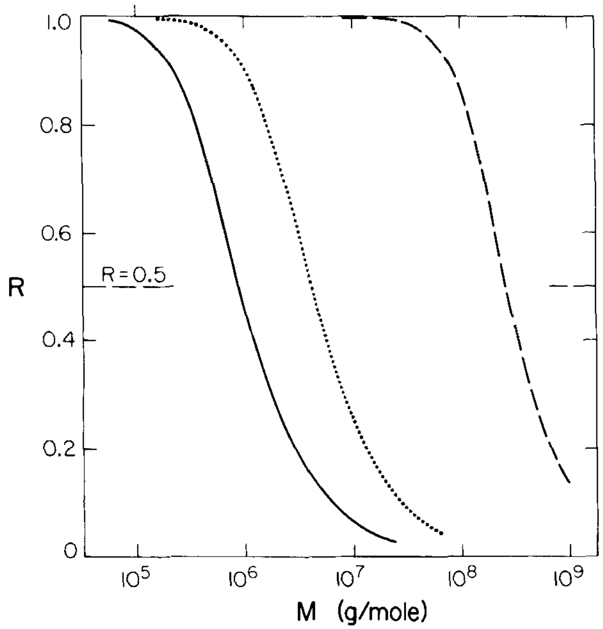

FIG. 4. Plot of R vs molecular weight M for cellulose acetate dissolved in *N*-methylformamide (solid line) and in dimethylsulfoxide (DMSO) (dotted line) and for polyethylene dissolved in *n*-hexane (dashed line). $E^r = 1.4 \times 10^7$ V/m; $\nu = 10{,}000$ Hz; $\rho_l = 0.75$.

$cm^3 = 1.66 \times 10^{-5}$ μm^3 for $\rho = 1$ g/cm^3 and $M = 10^7$ g/mol; this volume corresponds to an equivalent particle diameter of only 0.032 μm).

Finally, we consider the applicability of dielectrical FFF to aqueous suspensions and solutions which exhibit anomalously large complex permittivities in the kHz–MHz frequency range. The large permittivities of aqueous colloidal suspensions and polyelectrolyte solutions subject to low kHz-frequency fields are generally attributed to the polarization of the electrical double layers of the constituent particles (*23, 36–42*). In high kHz- to low MHz-frequency fields, these mixtures also exhibit a Maxwell-Wagner-type polarization due to charge buildup at the particle–fluid interface (*23*). Positive dielectrophoresis (inner-cylinder accumulation) is almost exclusively observed in both cases. Biological particles (e.g., cells, mitochondria, platelets, etc.) can exhibit positive or negative dielectrophoresis, depending on the field frequency, fluid conductivity, and other parameters (*23*).

General R values for colloidal particles and polyelectrolytes unfortunately cannot be calculated because particle permittivity ε_p^* is experimentally inaccessible (only the permittivity of the bulk solution or suspension can be measured) and theories for ε_p^* (*43, 44*) are inadequate (*37, 39–42*). Since practical considerations relating to Joule heating and thermal convection dictate the use of low-conductivity aqueous suspensions (or solutions), in which typically $\varepsilon_p^* \gg \varepsilon_f^*$, one important estimate of the force F on these particle types is made by equating the central expression in Eq. (21) to its maximum positive value, unity. (A similar approximation to the modulus of the complex expression in Eq. 12 gave close agreement between theoretical and experimental E^p values for an aqueous polystyrene suspension over the frequency range 10^3–10^8 Hz (*29*).) For this case λ^p, Eq. (13), assumes its maximum value and may be approximated as

$$\lambda^p = \frac{0.0551}{1 - \rho_1^2} \tag{22}$$

Based on Eq. (22), it is expected that the minimum R's for colloidal particles and polyelectrolytes suspended in low-conductivity aqueous media will be limited essentially by pearl-chain-formation parameter λ^p. The limitation is a serious one for reasonable ρ_1 values. For example, if $\rho_1 \geqslant 0.75$, then $R \geqslant 0.50$ and adequate particle retention is barely attainable.

CONCLUSIONS

The following assessments of the feasibility of dielectrical FFF are deduced from the study of Figs. 2–4 and the above discussion. First, dielectrical FFF shows considerable promise as a fractionation method for colloidal particles suspended in organic liquids of high dielectric constant (e.g., *N*-methylformamide, formamide, and DMSO). In such liquids, typical particles having minimum diameters of 0.06 μm or so can apparently be adequately retained ($R \leqslant 0.5$) using inner-cylinder field strengths limited by the mixtures' dielectric strengths ($E^d \simeq 10^6$ V/m).

Second, dielectrical FFF shows some promise for the retention of polar, high-molecular-weight polymers (e.g., $M \simeq 10^6$–10^7 g/mol) dissolved in polar liquids of high dielectric constant (e.g., *N*-methylformamide) using inner-cylinder field strengths equal to $E^d \simeq 10^7$ V/m. Nonpolar polymers of very large molecular weight (e.g., $M > 10^8$ g/mol) can in principle be adequately retained in nonpolar, low permittivity solvents, but few such polymers can in practice be synthesized or kept stably in solution because of viscous shearing. Dielectrical FFF thus appears to have little merit as a fractionation technique for nonpolar polymers dissolved in nonpolar solvents.

Finally, pearl-chain formation in low-conductivity aqueous colloidal suspensions and polyelectrolytes sets a lower limit on R of about 0.5 in practical ANNC systems ($\rho_l \geqslant \sim 0.7$), consequently making dielectrical FFF an ineffective fractionating method for such materials. Aqueous suspensions of biological particles which exhibit negative dielectrophoresis, however, might be adequately fractionated by dielectrical FFF; this possibility should be assessed experimentally.

Returning to the promising case of organic suspensions, we note that there are a number of similarities between dielectrical FFF and sedimentation FFF, which has been particularly effective in resolving and characterizing aqueous suspensions. Most generally, the limiting value of the mass-based selectivity of dielectrical FFF is predicted to be unity, a relatively high value identical to the limiting selectivity of sedimentation FFF (*45*). In addition, the dielectric constant of the suspending medium can be manipulated in much the same way and for essentially the same purpose in dielectrical FFF as the density of the suspending medium is manipulated in sedimentation FFF. In the latter case, runs made at different carrier densities can be used to characterize particle density as well as size, thus reflecting on the chemical composition of the particulate material (*46*). In the case of dielectrical FFF, successive runs with carriers of different dielectric constant should serve to identify the dielectric constant of the fractionated particles, which will again relate to the chemical composition of those particles. This approach has considerable potential for unraveling both the chemical nature and the size distribution of complex suspensions of colloidal particles in organic media.

The choice of channel dimensions in dielectrical FFF would be subject to many of the same compromises as those dictating channel dimensions in other forms of FFF. For particles with marginal retention, there is generally an advantage to increased channel thickness as shown by Eq. (7). However, for particles retained at the outside wall, this advantage is soon lost, either because the inside cylinder radius must become increasingly small and the limiting field strength at r_1 reduces that available at r_2 (see Eq. 6), or because r_2 is expanded and the nonuniformity in the field is compromised. However, more generally, large w values are expected to be disadvantageous because of sample dilution effects, a propensity toward convection, increased heat buildup in the channel which further aggravates convection, and an increased time necessary for initial particle relaxation.

With respect to the latter point, we note that in calculating R from Eq. (14), it was assumed that the component particles had, under the influence of force F, formed or relaxed into a steady-state particle cloud, as described in the Introduction. The dielectrical FFF relaxation time τ required to establish this steady-state distribution is (*24*)

$$\tau = \frac{r_2^2}{8D\rho_1^2}\lambda(1 - \rho_1^2)(1 - \rho_1^4) \tag{23}$$

where D is the species' diffusion coefficient. To insure formation of the steady-state layer, a stop-flow procedure should be used in which the electrical field is applied for a time $\geqslant \tau$ before the carrier fluid is pumped through the channel.

Finally, while this paper focuses on the use of dielectrophoresis in the so-called normal mode of operation of FFF, in which particles accumulate at one wall, dielectrophoretic forces might be similarly useful in developing hyperlayer FFF techniques, where particles are focused into thin layers (hyperlayers) within the channels (*10*). We have already noted the use of dielectric levitation; the levitation process, in which particles are held free from any containment surface, has the potential for forming the necessary hyperlayers within FFF channels. This approach merits further investigation.

SYMBOLS

a	particle radius
ANNC	annular channel
D	diffusion coefficient of species
DMSO	dimethylsulfoxide
E	electric field strength
E_1	maximum E value at inner cylinder of ANNC
E^d	threshold E value for dielectric breakdown
E^p	threshold E value for pearl-chain formation
E_{rms}	root-mean-square value of E
E_s	amplitude of E
E^t	threshold E value formation
F	dielectrophoretic force
FFF	field-flow fractionation
g	function defined by Eq. (4)
k	Boltzmann's constant
M	molecular weight of polymer

MEK	methyl ethyl ketone
OPPC	open parallel-plate channel
q	generalized coordinate
r	radial coordinate
r_1	inner radius of ANNC
r_2	outer radius of ANNC
R	gas constant
R	retention ratio
R_{in}	inner-wall retention ratio
R_{out}	outer-wall retention ratio
t	time
T	absolute temperature
u	$\alpha r_2^2/r^2$
V	particle volume
w	channel thickness
W	work required to transport a particle across the channel
α	$\rho_1^2/(\lambda(1 - \rho_1^2))$
ε_f^*	complex electrical permittivity of fluid
ε_p^*	complex electrical permittivity of particle
ε_f	electrical permittivity of fluid
ε_p	electrical permittivity of particle
θ	$(1 - \rho_1^2)/\ln \rho_1$
θ'	coefficient in Eq. (1) equal to 0.5
λ	$kT/\lvert W\rvert$
λ^d	threshold λ for dielectric breakdown
λ^p	threshold λ for pearl-chain formation
λ^t	threshold λ defined by $E_1 = E^t$
ν	frequency of electric field
ρ	density of polymer
ρ_1	r_1/r_2
σ_f	electrical conductivity of fluid
σ_p	electrical conductivity of particle
τ	relaxation time
τ_f	time constant defined by Eq. (2)
ϕ	$1 + \rho_1^2 + \theta$
ω	angular frequency of E

Acknowledgments

This material is based upon work supported by the National Science Foundation under Grant CHE82-18503. JMD recognizes support from the University of Utah Research Committee. The authors thank Dr Art

Janata of the University of Utah and Dr Kent Pollock of the Oklahoma State University for helpful discussions.

REFERENCES

1. J. C. Giddings, *Sep. Sci. Technol., 19,* 831 (1984).
2. J. C. Giddings, M. N. Myers, and K. D. Caldwell, *Ibid., 16,* 549 (1981).
3. J. C. Giddings, *Anal. Chem., 53,* 1170A (1981).
4. Y. S. Gao, K. D. Caldwell, M. N. Myers, and J. C. Giddings, *Macromolecules 18,* 1272 (1985).
5. C. R. Yonker, K. D. Caldwell, and J. C. Giddings, *J. Virol., 11,* 145 (1985).
6. L. F. Kesner, K. D. Caldwell, M. N. Myers, and J. C. Giddings, *Anal. Chem., 48,* 1834 (1976).
7. S. L. Brimhall, M. N. Myers, K. D. Caldwell, and J. C. Giddings, *J. Polym. Sci., Polym. Lett. Ed., 22,* 339 (1984).
8. T. C. Schunk, J. Gorse, and M. F. Burke, *Sep. Sci. Technol., 19,* 653 (1984).
9. J. C. Giddings and S. L. Brantley, *Ibid., 19,* 631 (1984).
10. J. C. Giddings, *Ibid., 18,* 765 (1983).
11. J. Janca and J. Chmelik, *Anal. Chem., 56,* 2481 (1984).
12. I. J. Lin, B. Z. Kaplan, and Y. Zimmels, *Sep. Sci. Technol., 18,* 683 (1983).
13. I. J. Lin and L. Benguigui, *Sep. Purif. Methods, 10,* 53 (1981).
14. K. Kaler and H. A. Pohl, *J. Biol. Phys., 8,* 18 (1980).
15. T. B. Jones and G. A. Kallio, *J. Electrost., 6,* 207 (1979).
16. L. Benguigui and I. J. Lin, *J. Appl. Phys., 49,* 2536 (1978).
17. H. A. Pohl, *Ibid., 29,* 1182 (1958).
18. H. A. Pohl and J. P. Schwar, *Ibid., 30,* 69 (1959).
19. H. A. Pohl and C. E. Plymale, *J. Electrochem. Soc., 107,* 390 (1960).
20. R. H. Kirchoff and A. Handi, *Ibid., 120,* 80 (1973).
21. I. J. Lin and L. Benguigui, *Sep. Sci. Technol., 17,* 645 (1982).
22. L. Benguigui and I. J. Lin, *Ibid., 17,* 1003 (1982).
23. H. A. Pohl, *Dielectrophoresis,* Cambridge University Press, Cambridge, 1978.
24. J. M. Davis and J. C. Giddings, *J. Phys. Chem., 89,* 3398 (1985).
25. K. Pollock, Oklahoma State University, Personal Communication, 1985.
26. L. Benguigui and I. J. Lin, *J. Appl. Phys., 53,* 1141 (1982).
27. F. A. Sauer, in *Coherent Excitations in Biological Systems* (H. Fröhlich and F. Kremer, eds.), Springer-Verlag, Berlin, 1983.
28. M. Saito and H. P. Schwan, in *Biological Effects of Microwave Radiation,* Vol. 1 (M. F. Peyton, ed.), Plenum, New York, 1960.
29. H. P. Schwan and L. D. Sher, *J. Electrochem. Soc., 116,* 22C (1969).
30. G. Schwarz, M. Saito, and H. P. Schwan, *J. Chem. Phys., 43,* 3562 (1965).
31. M. Saito, H. P. Schwan, and G. Schwarz, *Biophys. J., 6,* 313 (1966).
32. J. A. Riddick and W. B. Bunger, *Organic Solvents: Physical Properties and Methods of Purification,* Wiley-Interscience, New York, 1970.
33. J. Brandrup and E. H. Immergut (eds.), *Polymer Handbook,* 2nd ed., Wiley-Interscience, New York, 1975.
34. R. E. Bolz and G. L. Tuve (eds.), *CRC Handbook of Tables for Applied Engineering Science,* Chemical Rubber Company, Cleveland, 1970.
35. T. J. Gallagher, *Simple Dielectric Liquids: Mobility, Conduction, and Breakdown,* Clarendon Press, Oxford, 1975.

36. H. P. Schwan, *Adv. Biol. Med. Phys., 4,* 147 (1957).

37. S. S. Dukhin, and V. N. Shilov, *Dielectric Phenomena and the Double Layer in Disperse Systems and Polyelectrolytes,* Wiley, New York, 1974.

38. J. B. Hasted, *Aqueous Dielectrics,* Chapman and Hall, London, 1973.

39. S. S. Dukhin, *Surf. Colloid Sci., 3,* 83 (1973).

40. J. Lyklema, S. S. Dukhin, and V. N. Shilov, *J. Electroanal. Chem., 143,* 1 (1983).

41. M. Fixman, *J. Chem. Phys., 78,* 1493 (1983).

42. M. Fixman, *Ibid., 72,* 5177 (1980).

43. J. M. Schurr, *J. Phys. Chem., 68,* 2407 (1964).

44. G. Schwarz, *Ibid., 66,* 2636 (1962).

45. M. N. Myers and J. C. Giddings, *Anal. Chem., 54,* 2284 (1982).

46. J. C. Giddings, G. Karaiskakis, and K. D. Caldwell, *Sep. Sci. Technol., 16,* 607 (1981).

Received by editor January 17, 1986